

Comparison of two generation-recombination terms in the Poisson-Nernst-Planck model

*Original*

Comparison of two generation-recombination terms in the Poisson-Nernst-Planck model / I., Lelidis; Barbero, Giovanni; A., Sfarna. - In: THE JOURNAL OF CHEMICAL PHYSICS. - ISSN 0021-9606. - 137:(2012), p. 154104.  
[10.1063/1.4757020]

*Availability:*

This version is available at: 11583/2503437 since:

*Publisher:*

AIP American Institute of Physics

*Published*

DOI:10.1063/1.4757020

*Terms of use:*

This article is made available under terms and conditions as specified in the corresponding bibliographic description in the repository

*Publisher copyright*

(Article begins on next page)

## Comparison of two generation-recombination terms in the Poisson-Nernst-Planck model

I. Lelidis, G. Barbero, and A. Sfarna

Citation: *The Journal of Chemical Physics* **137**, 154104 (2012); doi: 10.1063/1.4757020

View online: <http://dx.doi.org/10.1063/1.4757020>

View Table of Contents: <http://scitation.aip.org/content/aip/journal/jcp/137/15?ver=pdfcov>

Published by the [AIP Publishing](#)

---

### Articles you may be interested in

[Independence of the effective dielectric constant of an electrolytic solution on the ionic distribution in the linear Poisson-Nernst-Planck model](#)

*J. Chem. Phys.* **141**, 084505 (2014); 10.1063/1.4893712

[Measurement of the impedance of aqueous solutions of KCl: An analysis using an extension of the Poisson-Nernst-Planck model](#)

*Appl. Phys. Lett.* **105**, 022901 (2014); 10.1063/1.4890386

[Note: Recombination of H<sup>+</sup> and OH<sup>-</sup> ions along water wires](#)

*J. Chem. Phys.* **139**, 036102 (2013); 10.1063/1.4811294

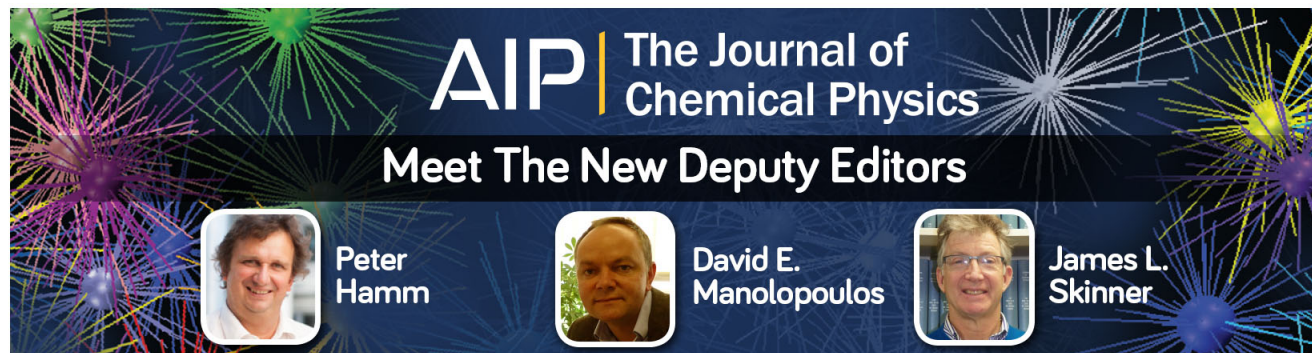
[Similarities and differences among the models proposed for real electrodes in the Poisson-Nernst-Planck theory](#)

*J. Chem. Phys.* **136**, 084705 (2012); 10.1063/1.3686767

[Electrical impedance of an electrolytic cell in the presence of generation and recombination of ions](#)




*J. Chem. Phys.* **132**, 224901 (2010); 10.1063/1.3447893

---



**AIP** | The Journal of  
Chemical Physics

### Meet The New Deputy Editors

|   |                   |   |                              |   |                         |
|---|-------------------|---|------------------------------|---|-------------------------|
|  | <b>Peter Hamm</b> |  | <b>David E. Manolopoulos</b> |  | <b>James L. Skinner</b> |
|---|-------------------|---|------------------------------|---|-------------------------|

## Comparison of two generation-recombination terms in the Poisson-Nernst-Planck model

I. Lelidis,<sup>1,2,3</sup> G. Barbero,<sup>2</sup> and A. Sfarna<sup>1</sup>

<sup>1</sup>*Solid State Section, Department of Physics, University of Athens, Panepistimiopolis, Zografos, Athens 157 84, Greece*

<sup>2</sup>*Department of Applied Science and Technology, Politecnico di Torino, Corso Duca degli Abruzzi 24, 10129 Torino, Italy*

<sup>3</sup>*Université de Picardie Jules Verne, Laboratoire de Physique des Systèmes Complexes, 33 rue Saint-Leu 80039, Amiens, France*

(Received 26 June 2012; accepted 18 September 2012; published online 15 October 2012)

Two phenomenological forms proposed to take into account the generation-recombination phenomenon of ions are investigated. The first form models the phenomenon as a chemical reaction, containing two coefficients describing the dissociation of neutral particles in ions, and the recombination of ions to give neutral particles. The second form is based on the assumption that in thermodynamical equilibrium, a well-defined density of ions is stable. Any deviation from the equilibrium density gives rise to a source term proportional to the deviation, whose phenomenological coefficient plays the role of a life time. The analysis is performed by evaluating the electrical response of an electrolytic cell to an external stimulus for both forms. For simplicity we assume that the electrodes are blocking, that there is only a group of negative and positive ions, and that the negative ions are immobile. For the second form, two cases are considered: (i) the generation-recombination phenomenon is due to an intrinsic mechanism, and (ii) the production of ions is triggered by an external source of energy, as in a solar cell. We show that the predictions of the two models are different at the impedance as well as at the admittance level. In particular, the first model predicts the existence of two plateaux for the real part of the impedance, whereas the second one predicts just one. It follows that impedance spectroscopy measurements could give information on the model valid for the generation-recombination of ions. © 2012 American Institute of Physics. [<http://dx.doi.org/10.1063/1.4757020>]

### I. INTRODUCTION

The dielectric properties of electrolytic cells strongly depend on the actual bulk density of ions, when probed by an external electric field in the low frequency region. The influence of the ions on the electrical response of a cell can be described using the equations of continuity for the anions and cations, and the equation of Poisson for the actual potential across the cell. This theoretical approach, known as the Poisson-Nernst-Planck (PNP) model, has been discussed in details long ago by Macdonald.<sup>1</sup> The simple case where the impurities producing the ions are completely dissociated is a good approximation of the real problem, only for low enough bulk density of ions. In this framework, the recombination of ions of opposite sign can be neglected since the probability of a collision between ions is very small.<sup>2</sup> When the bulk density of ions is not negligible, a term taking into account the generation-recombination (G-R) effect of ions has to be introduced in the model.

In the first attempt,<sup>3,4</sup> devoted to the generalization of the PNP model to account for the G-R effect, has been assumed that the ions are generated by impurities dissolved in the dielectric liquid according to a reaction of the form  $A = B^+ + C^-$ , where  $A$  is the density of neutral particles,  $B^+$  and  $C^-$  are the actual density of positive and negative ions, respectively. This reaction is characterized by two coefficients describing the generation (dissociation of  $A$ ) and the recombina-

tion (association of  $B^+$  with  $C^-$ ) of ions (ABC-source). Later on, the problem has been reconsidered by other researchers for different reasons.<sup>5,6</sup>

Recently, Bisquert proposed a theory for the ac impedance of electron diffusion and recombination in restricted geometry<sup>7</sup> introducing the G-R effect by a source term of the type  $\mathcal{S} = -k(N - N_0)$ , where  $N_0$  is the bulk density of ions in thermodynamical equilibrium, and  $N$  is the actual ionic concentration. According to this G-R term, whenever the local ionic concentration fluctuates from its equilibrium value, ionic recombination or generation increases to establish the original equilibrium value. This type of source term can further describe the generation of ions induced by an external source of energy that interacts with some kind of molecules dispersed in the liquid under consideration. From this point of view, the source term to introduce in the continuity equation is of the type  $\mathcal{S} = h - kN$ , where  $h$  is related to the generation of ions and  $k$  to their recombination.<sup>8-12</sup> At thermodynamical equilibrium  $\mathcal{S} = 0$  and  $N_0 = h/k$ . For small variations of  $N$  due to the presence of an external electric field or the confinement of the liquid, the term source  $\mathcal{S}$  can be rewritten as  $\mathcal{S} = -k(N - N_0)$ , having the same form as the term proposed in Ref. 7. Finally, note that, in the approach of Macdonald (ABC-source) the probability of association is quadratic in the concentration of the dissociated molecules, i.e., the reaction rate is of second-order, while in the approach proposed by Bisquert the reaction rate is linear (L-source).

The latter assumption is the usual one in irreversible thermodynamics.

In the present paper, our aim is to compare the influence of the two types of source term on the impedance of a cell filled with a liquid that contains impurities dissociable to ions. Therefore, we first solve the PNP model with a L-source term to obtain the impedance of a cell. Once we evaluate the spectra of the resistance, reactance, conductance, and susceptance, we compare the predictions of the L-source model with those deduced with the ABC-source model discussed in Refs. 1, 3, 5, and 6. We deduce that (i) the two models are not equivalent, and (ii) the impedance spectroscopy can distinguish between the two models and give information on the actual model for the generation-recombination phenomenon. In our analysis we assume that: (a) the cell is in the shape of a slab, in such a manner to reduce the problem to one-dimensional problem, (b) the electrodes are perfectly blocking, and (c) only the positive ions are mobile. Third hypothesis implies that we consider a medium which is like a polymer, with the negative ions stuck on the polymer chains, as in gels.<sup>13</sup>

As stated above, in our analysis we assume that the electrodes are perfectly blocking, and hence the electrical current in the external circuit is just a displacement current. Hence, the proposed model works reasonably well for cell limited by gold electrodes. In the case where the electrodes are not blocking, the analysis is more complicated because the current density of positive and negative ions do not vanish on the electrode. In this framework, to solve the bulk equations of the PNP model are necessary new boundary conditions for the current density of ions on the electrode. The boundary conditions proposed to take into account the partial blocking character of the electrodes have been recently discussed in Ref. 14, where it is shown that this property is responsible, in the low frequency region of the spectrum of a new plateau in the real part of the impedance of the cell. Since also the G-R effect is responsible for a similar effect, to avoid confusion, we limit the analysis to the case where the plateau in the dc limit is just due to the G-R effect. For the same reason we assume that only one group of ion is present, and only the positive ions are moving. In fact, if the mobilities of the ions are different,<sup>15</sup> or if two or more groups of ions are present,<sup>16</sup> in the low frequency limit a new plateau appears.

## II. ELECTRIC IMPEDANCE WITH AN L-SOURCE TERM

As discussed above, the PNP model is based on the differential equations representing the conservation of the positive and negative ions (continuity equations), and the relation between the electric field and the electrical charges (equation of Poisson).<sup>17</sup> The boundary conditions on the electrical potential simply state that the actual potential on the electrodes has to coincide with the one imposed by the external power supply. On the contrary, the boundary conditions on the current densities depend on the nature of the electrodes. If the electrodes are perfectly blocking, as considered in our paper, the current densities have to vanish on the electrodes. We assume that there are only two groups of ions, one positive and one negative. Let  $q$  indicate the modulus of the electrical

charge of the ions,  $\varepsilon$  the dielectric constant of the medium in which are dispersed the ions,  $D$  is the diffusion coefficient of the ions in the considered medium, and  $N_0$  is the actual bulk density of ions in thermodynamical equilibrium. Finally, we assume that the liquid is not dispersive in the considered frequency region. Therefore,  $\varepsilon$  can be considered frequency independent. Any dispersion is due to the influence of the ions on the response of the cell to the external stimulus.

The applied voltage is supposed harmonic,  $V(t) = V_0 \exp(i\omega t)$ , with a small enough amplitude,  $V_0$ , for the fundamental equations of the problem can be linearized.<sup>18</sup> For a cell in the shape of a slab of thickness  $d$  and electrode surface area  $S$ , the electrical impedance in absence of any source term is given by<sup>6</sup>

$$Z = \frac{d\beta_0(-1 + \Lambda^2\beta_0^2) + 2 \tanh(\beta d/2)}{i\varepsilon\Lambda^2\omega\beta_0^3 S}, \quad (1)$$

where  $\Lambda = \sqrt{\varepsilon k_B T / (N_0 q^2)}$  is the Debye length of the mobile ions, and  $\omega = 2\pi f$  is the angular frequency. The complex wave vector  $\beta_0$  is given by

$$\beta_0 = \frac{1}{\Lambda} \sqrt{1 + i \frac{\omega}{\omega_D}}, \quad (2)$$

where  $\omega_D = D/\Lambda^2$  is the Debye relaxation frequency. By taking into account the expression of  $\beta_0$  given by Eq. (2), Eq. (1) giving the impedance of the cell can be rewritten as

$$Z = -i \frac{2}{\omega\varepsilon\beta_0^2 S} \left\{ \frac{1}{\Lambda^2\beta_0} \tanh(\beta_0 d/2) + i \frac{\omega d}{2D} \right\}. \quad (3)$$

Introducing the L-source term discussed in Ref. 7, we obtain for the impedance of the cell (see Appendix A for the detailed derivation of the impedance) the following expression:

$$Z = \frac{d\beta(-1 + \Lambda^2\beta^2) + 2 \tanh(\beta d/2)}{i\varepsilon\Lambda^2\omega\beta^3 S}, \quad (4)$$

i.e., the impedance is still given by Eq. (1) but the complex wave vector  $\beta_0$  is renormalized to

$$\beta = \frac{1}{\Lambda} \sqrt{1 + \kappa + i \frac{\omega}{\omega_D}}, \quad (5)$$

where  $\kappa = k/\omega_D$ , as discussed in Appendix B.

As it is clear from Eqs. (4) and (5), the presence of the L-source term modifies the frequency dependence of the electrical impedance, mainly in the frequency range where  $\kappa \sim \omega/\omega_D$ , i.e.,  $\omega \lesssim \kappa\omega_D$ . On the contrary, in the high frequency range, when  $\omega \gg \kappa\omega_D$  its effect is negligible. This is consistent with the meaning of  $k$  that represents a kind of lifetime of the free charges.<sup>7</sup>

We further investigate the behavior of the impedance by proceeding to numerical calculations. The ions are assumed monovalent,  $q = 1.6 \times 10^{-19}$  A s,  $K_B T/q = 25$  mV,  $\varepsilon = 80 \times \varepsilon_0$ ,  $D = 10^{-10}$  m<sup>2</sup>/s,  $N_0 = 10^{22}$  m<sup>-3</sup>, as for ions in a water solution weakly ionized.<sup>19</sup> With these values  $\Lambda = 0.105$   $\mu$ m and  $\omega_D \sim 9$  KHz. The geometrical parameters of the cell are taken  $d = 0.5 \times 10^{-3}$  m and  $S = 10^{-4}$  m<sup>2</sup>.

Figure 1 shows the spectra of the real (a),  $R = \text{Re}[Z]$ , and imaginary (b),  $X = \text{Im}[Z]$ , part of the electrical impedance of the cell,  $Z$ , for three values of  $\kappa = 0, 0.1, 1$ . The quantities

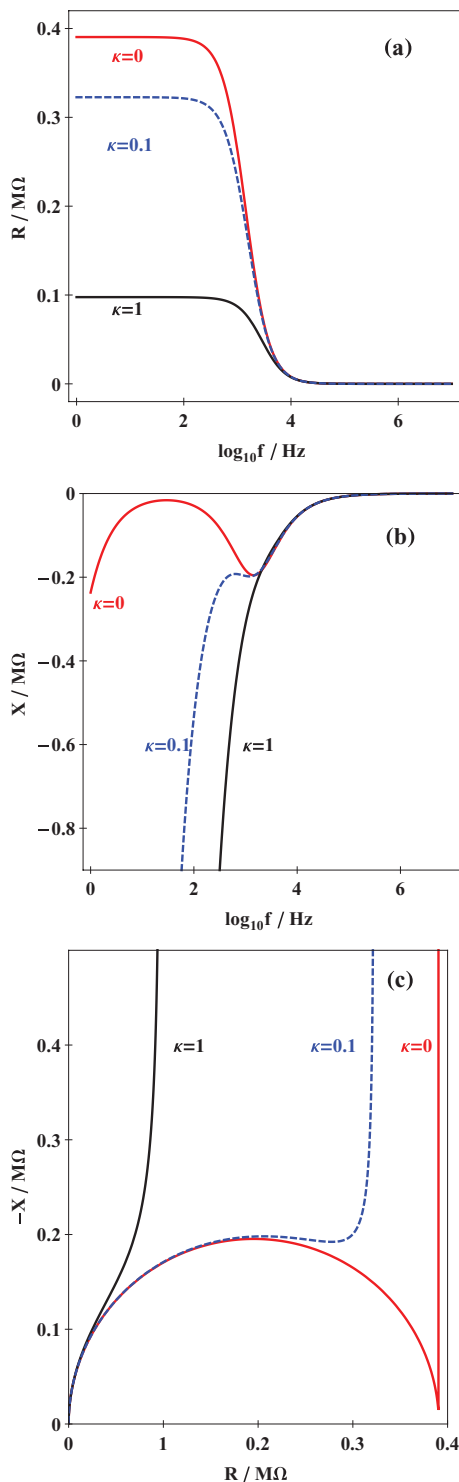


FIG. 1. Spectra of the resistance  $R = \text{Re}[Z]$ , (a), reactance  $X = \text{Im}[Z]$ , (b), and Nyquist plot, (c), for: full dissociation  $\kappa = 0$ , moderate recombination  $\kappa = 0.1$ , and large recombination  $\kappa = 1$ . For the numerical calculations, we assume that the ions are monovalent,  $q = 1.6 \times 10^{-19}$  A s,  $K_B T/q = 25$  mV,  $\varepsilon = 80 \times \varepsilon_0$ ,  $D = 10^{-10}$  m<sup>2</sup>/s,  $N_0 = 10^{22}$  m<sup>-3</sup>, and hence  $\Lambda = 0.105$   $\mu\text{m}$  and  $\omega_D \sim 9$  KHz. The geometrical parameters of the cell are  $d = 0.5 \times 10^{-3}$  m and  $S = 10^{-4}$  m<sup>2</sup>.

$R$  and  $X$  represent the resistance and reactance, respectively, in the series representation of the cell. The case  $\kappa = 0$  corresponds to full dissociation,  $\kappa = 0.1$  to moderate recombination, and  $\kappa = 1$  to large recombination. From Fig. 1(a)

it follows that by increasing  $\kappa$  the value of the plateau decreases monotonically, while the relaxation frequency of Debye seems almost fixed. Figure 1(b) shows that the influence of  $\kappa$  on the  $X(f)$  spectrum is restricted in a frequency range close to  $\omega_D$ . As  $\kappa$  increases, the position of the maximum of the reactance moves towards the high frequency region and disappears when  $\kappa$  reaches a critical value. Figure 1(c) is reported the parametric representation of  $X$  versus  $R$  (Nyquist diagram) with parameter the frequency of the applied external voltage.

Figure 2 shows the real (a),  $G$ , and the imaginary (b) part,  $B$ , of the admittance of the cell  $Y = 1/Z$ . They are related to the conductance and susceptance of the cell in the parallel representation. For the conductance  $G$ , the influence of  $\kappa$  is important in the full frequency range. For the susceptance  $B$  on the contrary,  $\kappa$  plays an important role only in the frequency range close to  $\omega_D$ . Clearly, increasing  $\kappa$ , the maximum of  $B$  moves first to higher frequencies and disappears above some critical value of  $\kappa$ . Figure 2(c) represents the Nyquist diagram.

In the dc limit, by means of Eq. (4) we get that the resistance  $R$  and capacitance  $C = -1/(\omega X)$  tend to

$$R_0 = \frac{d}{\varepsilon \omega_D S} \frac{1}{(1 + \kappa)^2}, \quad (6)$$

$$C_0 = \varepsilon S \frac{(1 + \kappa)^{3/2}}{2\Lambda + d\kappa(1 + \kappa)^{1/2}}. \quad (7)$$

Equation (6) gives the  $\kappa$  dependence of the plateau of  $R_0$ . From Eqs. (6) and (7), we obtain in the  $\kappa \rightarrow 0$  limit

$$R_0 = \frac{d}{\varepsilon \omega_D S} \quad \text{and} \quad C_0 = \varepsilon \frac{S}{2\Lambda}, \quad (8)$$

whereas, in the opposite limit,  $\kappa \rightarrow \infty$ , we get

$$R_0 \rightarrow \frac{d}{\varepsilon \omega_D S} \kappa^{-2} \quad \text{and} \quad C_0 = \varepsilon \frac{S}{d}. \quad (9)$$

From Eqs. (8) and (9), one deduces that for small  $\kappa$  the capacitance of the cell is reduced to the series of two capacitances related to the layers of Debye. In the opposite limit of large  $\kappa$ , the cell behaves as a pure condenser without losses. The  $0 \leq \kappa \leq 1$  dependence of  $R_0$  and  $C_0$  is reported in Figs. 3(a) and 3(b), respectively. Their behavior is monotonic with  $\kappa$ .

### III. CHARACTERISTICS FREQUENCIES

As it follows from Fig. 1(b), the reactive part of the impedance of the cell shows a non-monotonic behavior in the frequency range  $\omega < \omega_D$  when  $\kappa$  is lower than a critical value. It is possible to obtain analytically the position of the maximum of the reactance  $X(\omega)$  in an approximate manner as follows. By means of Eq. (4), in the limit of  $d \gg \Lambda$ , one obtains for  $X(\omega)$  the expression

$$X = X_{-1} + X_1, \quad (10)$$

where  $X_{-1}$  and  $X_1$  are the terms in  $(\omega/\omega_D)^{-1}$  and in  $(\omega/\omega_D)$  obtained by expanding the imaginary part of  $Z$  in power series of  $\omega/\omega_D$ , valid for  $(\omega/\omega_D) < 1$ . If we look for the extremum



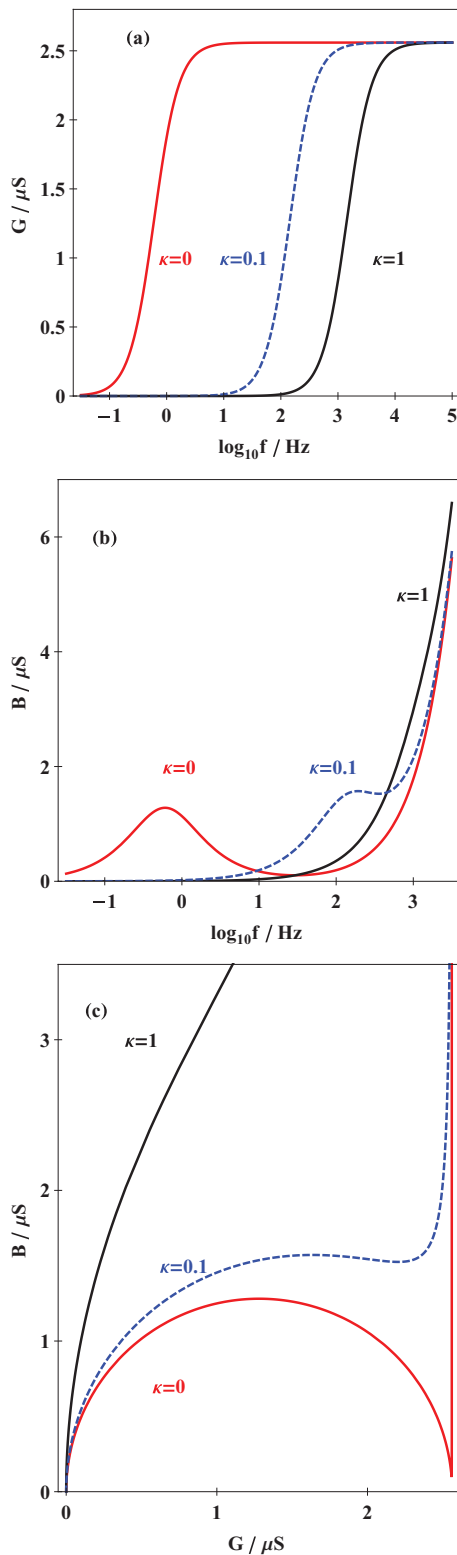


FIG. 2. Spectra of the real  $G = \text{Re}[Y]$ , (a), and imaginary  $B = \text{Im}[Y]$ , (b), parts of the admittance of the cell  $Y = 1/Z$  for  $\kappa = 0, 0.1, 1$ . Nyquist plot  $B = B(G)$ , (c). Numerical values used for the calculations are the same as in Fig. 1.

of  $X(\omega)$  given by Eq. (10), from the condition  $dX/d\omega = 0$  we get

$$\omega_X = \omega_D (1 + \kappa)^{3/4} \sqrt{2(\Lambda/d) + \kappa(1 + \kappa)}. \quad (11)$$

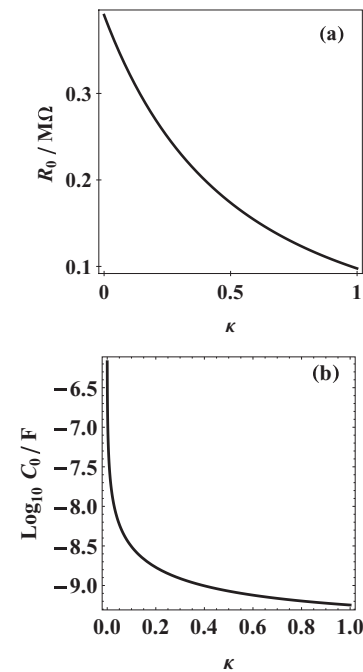


FIG. 3. Dependence of  $R_0$ , (a), and of  $C_0$ , (b), versus  $\kappa$ , when the ionic production in the medium is due to an internal mechanism. Numerical values used for the calculations are the same as in Fig. 1.

We observe that the same frequency is obtained by imposing the condition  $X_{-1} = X_1$ . From Eq. (11) in the limit of small  $\kappa$ , we obtain

$$\omega_X = \sqrt{2\frac{\Lambda}{d}} \omega_D + \frac{1}{4} \sqrt{2\frac{d}{\Lambda}} \omega_D \kappa. \quad (12)$$

The first contribution has been discussed recently for its practical importance to characterize a cell of electrolyte by means of the impedance spectroscopy.<sup>20</sup>

The same type of calculation can be done at the admittance level to derive the characteristic frequency of  $B = \text{Im}[Y]$ . In this case, we obtain

$$B = B_1 + B_3, \quad (13)$$

where  $B_1$  and  $B_3$  are the terms in  $\omega/\omega_D$  and in  $(\omega/\omega_D)^3$ , respectively, obtained by expanding in power series of  $\omega/\omega_D$  the quantity  $B = \text{Im}[Y]$ . By looking for the extremum for  $B$  given by Eq. (13), we obtain

$$\omega^* = \frac{1}{\sqrt{3}} \left\{ 2\frac{\Lambda}{d} + \kappa \left( 1 + \frac{\kappa}{2} \right) \right\} \omega_D. \quad (14)$$

On the contrary, by the condition  $B_1 = B_3$  we get

$$\omega_B = \left\{ 2\frac{\Lambda}{d} + \kappa \left( 1 + \frac{\kappa}{2} \right) \right\} \omega_D, \quad (15)$$

i.e.,  $\omega_B = \sqrt{3}\omega^*$ . By expanding  $\omega_B$  in power series of  $\kappa$ , we obtain

$$\omega_B = 2\frac{\Lambda}{d} \omega_D + \kappa \omega_D. \quad (16)$$

In Fig. 4 we show, dashed lines, the characteristics frequencies  $\omega_X$  and  $\omega_B$  versus  $\kappa$ , calculated from the approximated analytical expressions derived above, Eqs. (11) and (15), respectively. The continued lines represent

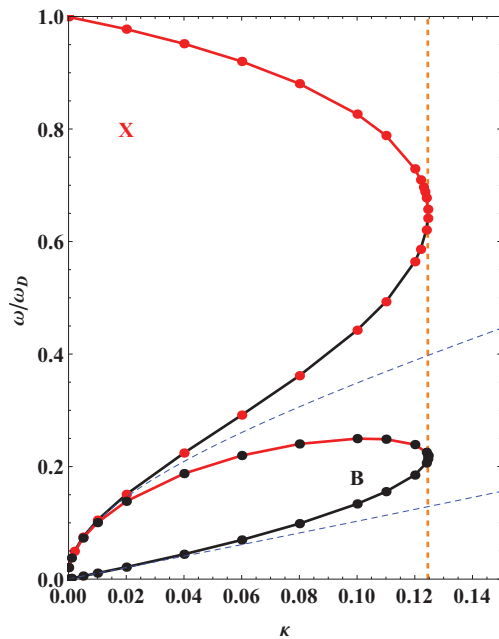


FIG. 4. Characteristic frequencies related to the extrema of  $X$  and  $B$ :  $\omega_X$  (upper dashed line) and  $\omega_B$  (lower dashed line), respectively, versus  $\kappa$ , calculated analytically. Vertical dashed line at the critical value  $\kappa_c = 0.1245$ . The continuous lines represent the position of minima and maxima of  $X$  (upper curve), and  $B$  (lower curve) calculated from numerical minimization of  $X$  and  $B$ , respectively. The lower branch of each curve corresponds to the locus of maxima for  $X$  and  $B$ . Numerical values used for the calculations are the same as in Fig. 1.

the locus of the extrema of the reactance and the admittance calculated by numerical minimization of the full expressions deduced from Eq. (4). The vertical dashed line is their common tangent at the critical value of  $\kappa_c = 0.1245$  above which  $B$  and  $X$  become monotonic functions of the frequency. At  $\kappa_c$  the relative maximum and minimum of each curve ( $X$  and  $B$ ) meet at an inflexion point above which they disappear. The approximated expression for  $\omega_X$  (upper dashed line) and  $\omega_B$  (lower dashed line) obtained analytically are valid only for low enough values of  $\kappa$ . Therefore for  $\kappa \lesssim 0.05$ , the characteristic frequencies can be calculated from the conditions  $X_{-1} = X_1$  and  $B_1 = B_3$ .

In the model described above,  $\tau = 1/k$  has the meaning of characteristic recombination time, and the parameter  $\kappa = k/\omega_D$  can be rewritten as  $\kappa = \tau_D/\tau$ , where  $\tau_D = \Lambda^2/D$  is the diffusion time. It is related to the time necessary to diffuse through a layer whose thickness is of the order of the Debye length. It follows that in the case of small recombination  $\tau \ll \tau_D$ . In the opposite case,  $\tau$  can be comparable with  $\tau_D$ .

Finally, because of recombination a second characteristic length enters the model, the recombination length  $\Lambda_R = \sqrt{D/2\pi k}$  that gives the average distance the ions diffuse before recombining. As far as  $\Lambda_R$  is similar or smaller than  $\Lambda$  the minimum of  $X$  should be visible, while for larger values it should be hidden from the created ions that diffuse at larger distances than Debye's length before recombining. According to the numerical minimization, above the critical recombination rate  $k_c = 1125.4$  Hz no minimum appears.

The latter value of  $k_c$  corresponds to the recombination length  $\Lambda_{R_c} = 0.119 \mu\text{m}$ , while the Debye length is  $\Lambda = 0.105 \mu\text{m}$ .

#### IV. ELECTRIC IMPEDANCE WITH AN ABC-SOURCE TERM

The case where the G-R effect is described by a reaction of the type  $A = B^+ + C^-$ , being  $B^+$  and  $C^-$  the positive and negative ions resulting from the decomposition of the neutral impurity  $A$ , has been extensively studied in the frame of the PNP model.<sup>4-6</sup> For convenience, in the following we briefly recall the main results reported in Ref. 6, relevant for the present analysis.

Let  $\mathcal{N}_d$ ,  $\mathcal{N}_n$ , and  $\mathcal{N}$  indicate the bulk densities of dissociable, of neutral, and of charged particles. In the thermodynamical equilibrium state, we have

$$\mathcal{N} + \mathcal{N}_n = \mathcal{N}_d \quad \text{and} \quad k_d \mathcal{N}_n = k_a \mathcal{N}^2, \quad (17)$$

where  $k_d$  and  $k_a$  are the dissociation and association coefficients, respectively. For a cell in the shape of a slab of thickness  $d$ , surface area  $S$ , and with perfectly blocking electrodes, the electrical impedance is given by

$$Z = -2 \frac{i}{\omega \varepsilon S \xi^2} \Upsilon \left\{ \frac{1}{\xi \bar{\lambda}^2} \tanh\left(\frac{\xi d}{2}\right) + i \frac{\omega d}{2D} \right\}, \quad (18)$$

where

$$\Upsilon = \frac{i\omega + k_d + 2k_a \mathcal{N}}{i\omega + k_d + k_a \mathcal{N}}, \quad (19)$$

$$\xi^2 = \frac{\Upsilon}{\bar{\lambda}^2} \left( 1 + i\omega \frac{\bar{\lambda}^2}{D} \right), \quad (20)$$

$$\bar{\lambda}^2 = \frac{\varepsilon k_B T}{\mathcal{N} q^2}. \quad (21)$$

Expression (18) generalizes Eq. (3) when the generation-recombination phenomenon is present, by simply rescaling Eq. (3) with the complex factor  $\Upsilon$ .

To numerically investigate the frequency dependence of the impedance, we use the same values for the constants entering the impedance expression as before, and  $k_a = 10^{-22} \text{ m}^3/\text{s}$ ,  $k_d = 1 \text{ s}^{-1}$ ,  $\mathcal{N}_d = 10^{24} \text{ m}^{-3}$ , as in Refs. 6 and 20.

In Figs. 5 and 6, we compare the predictions of the PNP model with G-R effect that is modeled by (i) an L-source term, with (ii) an ABC-source term. We assume that in thermodynamical equilibrium the number of ions is the same for the two cases. Since with the values of  $k_a$ ,  $k_d$ , and  $\mathcal{N}_d$  reported above, the bulk density of ions in thermodynamical equilibrium calculated from Eq. (17) is  $0.95 \times 10^{23} \text{ m}^{-3}$ ,<sup>6</sup> we assume, when considering the L-source term,  $N_0 = 0.95 \times 10^{23} \text{ m}^{-3}$ . Figure 5(a) shows that the  $R = R(f)$  for the L-source type (dashed line) has just one plateau, whose value depends on  $\kappa$ , whereas the ABC-source model predicts two plateaux, as discussed in details in Ref. 6. On the contrary, the reactance  $X = X(f)$  has the same behavior for both models, although the position of the minimum is located at different positions, as shown in Fig. 5(b). Similar conclusions can be

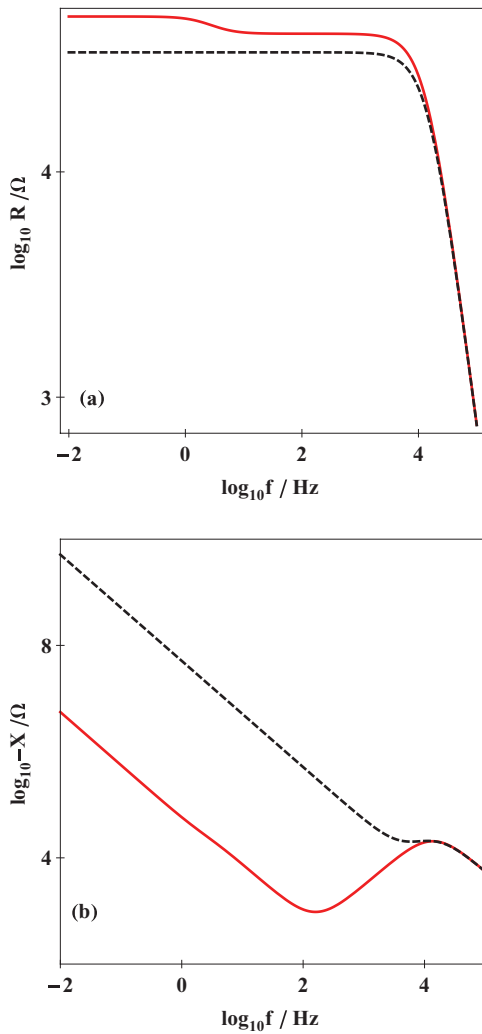


FIG. 5. Comparison of the predictions of the PNP model with an L-source term (dashed lines), and an ABC-source term (continuous lines).  $R(f)$ , (a),  $X(f)$ , (b). For the L-model the numerical values are the same considered in Fig. 1 with  $N_0 = 0.95 \times 10^{23} \text{ m}^{-3}$ . For the ABC-model  $k_d = 10^{-22} \text{ m}^3/\text{s}$ ,  $k_d = 1 \text{ s}^{-1}$ ,  $\mathcal{N}_d = 10^{24} \text{ m}^{-3}$  in such a manner that the bulk density of ions in thermodynamical equilibrium is the same for the two cases.

derived at the admittance  $Y$  level, as shown in Fig. 6, for its real  $G(f)$ , (a), and imaginary  $B(f)$ , (b), parts.

## V. INTERACTION WITH AN EXTERNAL SOURCE OF ENERGY

In Secs. II–III, we have considered the generation-recombination term in the form proposed by Bisquet.<sup>7</sup> As mentioned in the Introduction, a possible physical interpretation of this term could be the following: all the time the thermal density of ions is changed, recombination or dissociation takes place towards equilibrium. In a way, there is an optimum distance between the ions. If this distance is changed, the ions interact, via recombination or neutral particle dissociation to re-establish their optimum distance. From this point of view, the optimum distance is an internal property of the system. We consider now another situation. Let us assume that the density of particles that can give rise to ions, in condition of equilibrium, is  $\mathcal{N}_0$ . If we supply energy to the sample, for instance

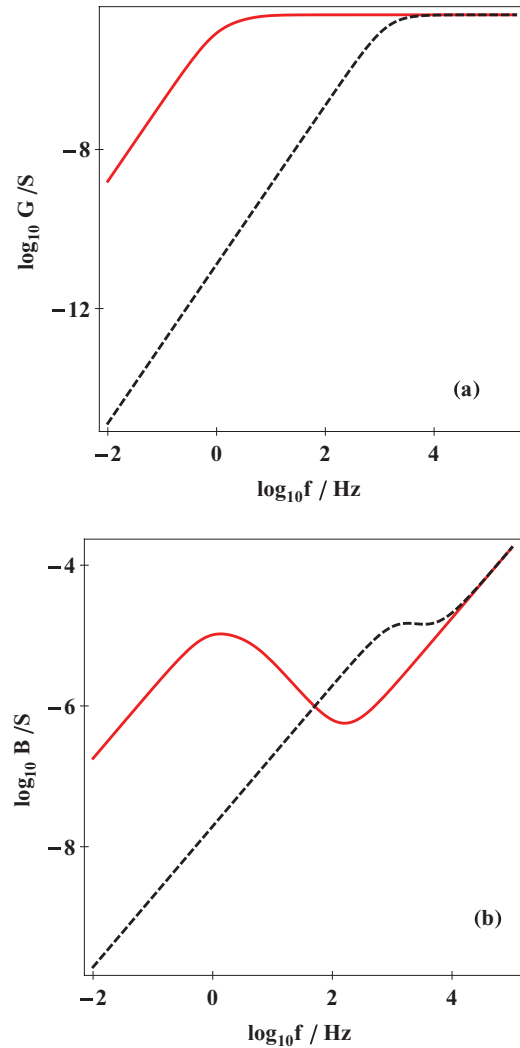


FIG. 6. Comparison of the predictions of the PNP model with an L-source term (dashed lines), and an ABC-source term (continuous lines).  $G(f)$ , (a),  $B(f)$ , (b). Numerical values used for the calculations are the same as in Fig. 5.

in the form of electromagnetic waves that interact with the dissociable particles, it is possible to generate ions.<sup>8–12</sup> If we assume that in the absence of external energy, the dissociable particles are stable, then the formation of ions is related to the external energy. In a first approximation the mechanism can be described by the equation

$$\frac{dN}{dt} = h - kN, \quad (22)$$

where  $h$  is related to the rate of ion creation per unit volume induced by the external energy supplied to the sample,  $k$  to the recombination rate of the ions, and  $N$  is the bulk density of ions. Equation (22) holds in the case where the diffusion of particles is negligible, i.e., for an infinite sample, and in absence of an external electric field, responsible for the drift of the ions. The solution of Eq. (22) is simply

$$N(t) = N_0(1 - e^{-kt}), \quad (23)$$

where  $N_0 = h/k \leq \mathcal{N}_0$ , and we have assumed that the energy has been sent on the sample at  $t = 0$ . From Eq. (23), it is clear that the meaning of  $\tau = 1/k$  is a characteristic recombination



time. For  $t \gg \tau$ ,  $N$  reaches the steady state value  $\tau h$ . In terms of  $N_0$  Eq. (22) can be rewritten as

$$\frac{dN}{dt} = -k(N - N_0) \quad (24)$$

as suggested in Ref. 7. Of course, in this case the meaning of  $k$  is different from the previous case. In fact, if the mechanism of production of ions is an internal mechanism,  $k$  just stabilizes the initial bulk density of ions, related, for instance, to thermal activated process. In this framework, for  $k \rightarrow 0$ , the recombination time tends to infinite, and we are in the situation of fully dissociated impurities. In the opposite limit of  $k \rightarrow \infty$ , the recombination time tends to zero, and we have no ions in the medium under consideration. These results are in agreement with the spectra presented in Figs. 1 and 3.

On the contrary, when Eq. (24) is related to the interaction with the external source of energy the role of  $k$  is different. In fact, in this case, as it is evident from Eq. (23), for  $k \rightarrow 0$  the number of ions is increasing linearly with  $t$ , up to  $\mathcal{N}_0$ . In the opposite case where  $k \rightarrow \infty$ ,  $N_0 = h/k \rightarrow 0$ , and we have no ions in the medium. In this limit the medium behaves as a pure insulator.

The analysis of this new point of view is of some importance, mainly in connection with the solar cells. To investigate the predictions of the model in the case where the ions are created from the interaction with the external source of energy, it is necessary to take into account that the bulk density of ions depends on  $k$ . Let us assume that the parameter  $h$  related to the production of ions from the external energy can be considered constant, and analyze the influence of  $k$  on the impedance of the sample. The equations reported above remain valid, but it is necessary to take into consideration that from  $N_0 = h/k$  it follows that  $\omega_D = D/\Lambda^2$  depends also on  $k$  according to the relation

$$\omega_D = \frac{\alpha}{k}, \quad \text{where} \quad \alpha = \frac{Dq^2h}{\varepsilon k_B T}, \quad (25)$$

i.e.,  $h$  changes the number  $N_0$  of dissociated particles in the thermodynamical state equilibrium. The quantity  $\kappa$  introduced above is now given by  $\kappa = k^2/\alpha$ .

The frequency dependence of the impedance is investigated numerically, keeping the same values for the constants as before, and by assuming for  $k \sim 10^4 \text{ s}^{-1}$ , as reported in Ref. 12, we get  $h = 10^{26} \text{ (s m}^3\text{)}^{-1}$ . In Fig. 7, we show the real, (a), and imaginary, (b), parts of the electrical impedance of the cell for three values of  $k$ , and the Nyquist diagram, (c), deduced by means of Eq. (4). As it is apparent from Fig. 7(a), the dependence of  $R$  versus the frequency of the external field is not monotonic with  $k$ . It is also clear from Fig. 7 that  $\omega_D$  decreases with  $k$  as predicted by Eq. (25). In Fig. 8, we show the dependence of  $R_0$ , (a), and of  $C_0$ , (b), versus  $k$ . As discussed above,  $R_0$  depends on  $k$  in non-monotonic manner. By means of Eq. (6), and taking into account Eq. (25),  $R_0$  can be written as

$$R_0(k) = \frac{\alpha}{\varepsilon S} \frac{k}{(\alpha^2 + k^2)^2}. \quad (26)$$

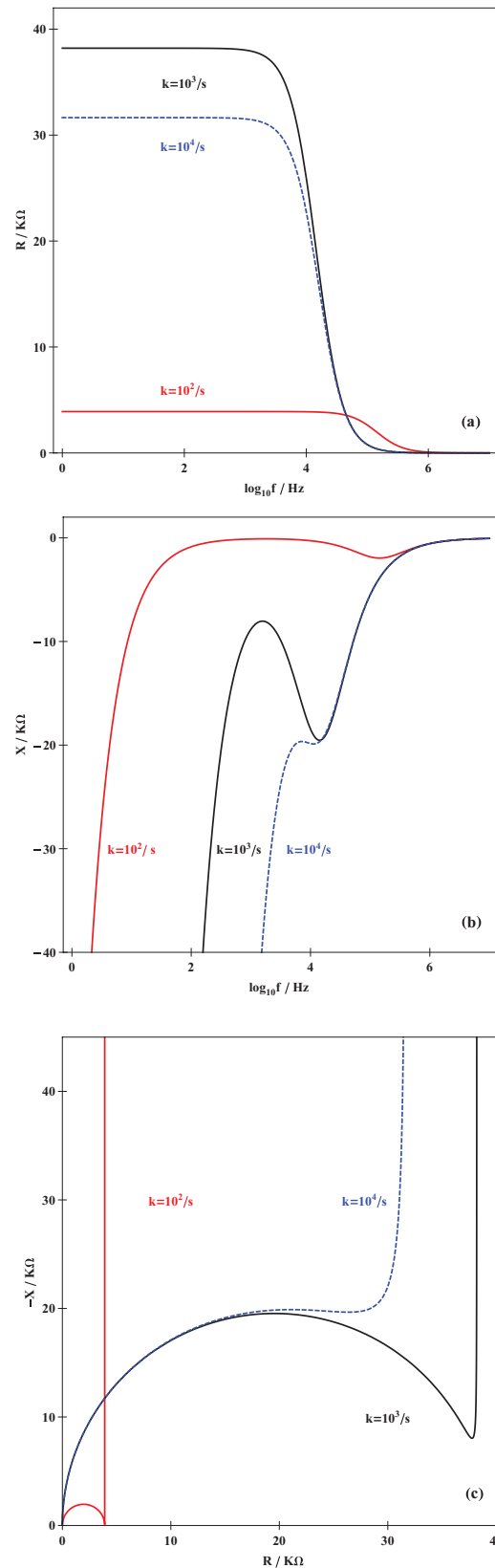


FIG. 7. Frequency dependence of the real, (a), and imaginary, (b), parts of the electrical impedance of the cell for three values of  $k$ , and Nyquist plot, (c), when the ions production in the medium is triggered by an external source of energy. For the numerical calculations, we assume that the ions are monovalent,  $q = 1.6 \times 10^{-19} \text{ A s}$ ,  $K_B T/q = 25 \text{ mV}$ ,  $\varepsilon = 80 \times \varepsilon_0$ ,  $D = 10^{-10} \text{ m}^2/\text{s}$ ,  $h = 10^{26} \text{ (s m}^3\text{)}^{-1}$ , and  $k = 10^2/\text{s}$ ,  $k = 10^3/\text{s}$ ,  $k = 10^4/\text{s}$ . The geometrical parameters of the cell are  $d = 0.5 \times 10^{-3} \text{ m}$  and  $S = 10^{-4} \text{ m}^2$ .

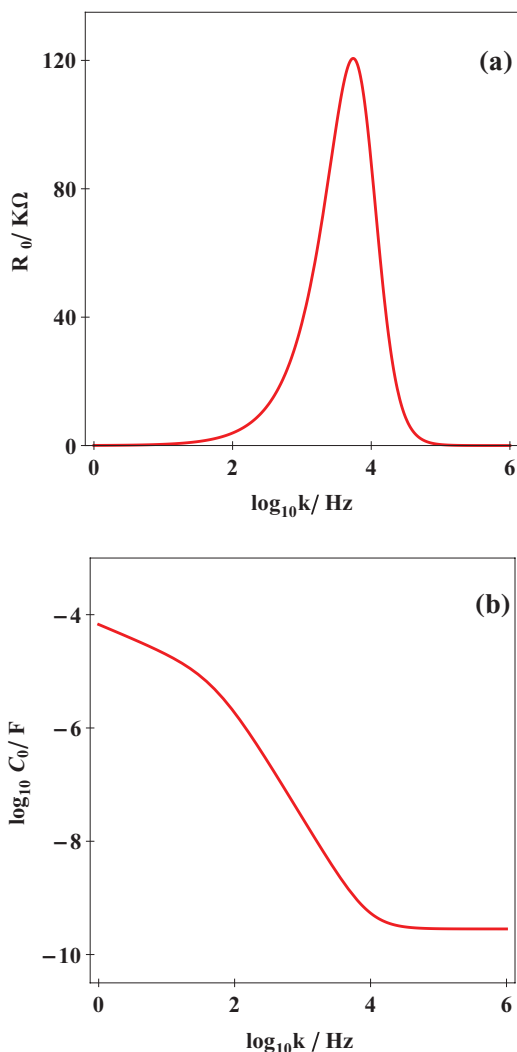


FIG. 8. Dependence of  $R_0$ , (a), and  $C_0$ , (b), versus  $k$ , when the ions production in the medium is controlled by an external source of energy. Numerical values used for the calculations are the same as in Fig. 7.

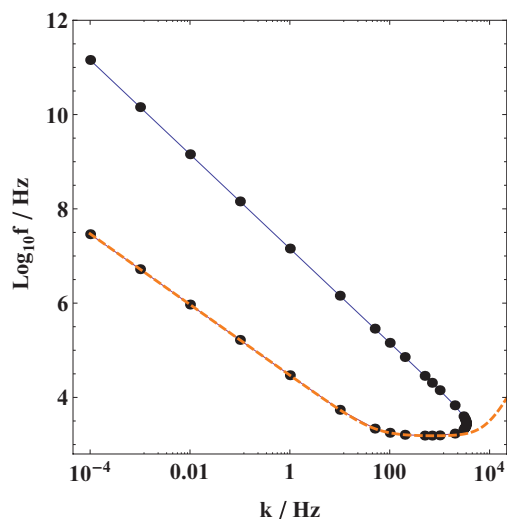


FIG. 9. The position of the extrema of  $X$  calculated numerically (continuous line) versus  $k$ , when the ions production in the medium is controlled by an external source of energy. The dashed line gives the approximated analytical prediction for the maxima position. Numerical values used for the calculations are the same as in Fig. 7.

The quantity  $R_0$  presents a maximum for  $k = \alpha/\sqrt{3}$ , where its value is

$$R_0(\alpha/\sqrt{3}) = \frac{3\sqrt{3}}{16\alpha^2\varepsilon S}. \quad (27)$$

Of course for  $k \rightarrow 0$ , the system behaves as a pure conducting system, and in the dc limit  $R_0 \rightarrow 0$  and  $C_0 \rightarrow \infty$ . In the opposite limit where  $k \rightarrow \infty$ , the medium is a true insulator, and  $R_0 \rightarrow 0$  and  $C_0 = \varepsilon S/d$ . Finally, Fig. 9 shows the position of the minimum and the maximum of  $X$  as function of  $k$ . The continuous line is calculated by numerical minimization of  $X$ . The dashed line represents the locus of the maxima of  $X$  given by the approximate analytical solution Eq. (12), taking into account Eq. (25).

## VI. CONCLUSIONS

We have considered the influence of the generation-recombination phenomenon on the spectra of the real and imaginary parts of the electrical impedance of an electrolytic cell. In the framework of the Poisson-Nernst-Planck model, we have compared two different sources that account for the G-R phenomenon: (i) the L-source model and (ii) the ABC-source model. The comparison has been performed between our results for the L-source model and the main predictions of the ABC-source model reported in Refs. 5 and 6. Our analysis has been performed for a cell in the shape of a slab with perfectly blocking electrodes, with the assumption that only the cations are mobile. Therefore, our predictions apply to a medium such as a polymer with anions stuck on the polymer chains. We have shown that the two model sources are not equivalent, and that the impedance spectroscopy measurements can give information on the actual model for the generation-recombination phenomenon. We have also investigated the case where the generation of ions is triggered by an external source of energy, and shown that one can control the number of dissociable particles at equilibrium. Finally, we introduced the characteristic length of recombination and shown its utility for the interpretation of the reactance and susceptance spectra.

## APPENDIX A: DERIVATION OF THE IMPEDANCE

The fundamental equations of the problem are the equation of continuity for the mobile ions

$$\frac{\partial N}{\partial t} = -D \frac{\partial}{\partial z} \left\{ \frac{\partial N}{\partial z} + \frac{qN}{K_B T} \frac{\partial V}{\partial z} \right\} - k(N - N_0), \quad (A1)$$

and the equation of Poisson for the actual electric potential in the cell

$$\frac{\partial^2 V}{\partial z^2} = -\frac{q}{\varepsilon}(N - N_0). \quad (A2)$$

Equation (A2) is valid under the hypothesis that the effective dielectric constant of the medium is position independent. This assumption is reasonable. In fact, since the density of ions is negligible with respect to that of the neutral particles of the liquid, their contribution to the effective dielectric constant can be neglected.<sup>2</sup> Consequently, there is not spatial

variation of  $\varepsilon$  due to the confinement of the ions close to the electrodes due to the applied potential.

We assume that the external potential is so small that  $n = N - N_0 \ll N_0$  and rewrite Eqs. (A1) and (A2) in the form

$$\frac{\partial n}{\partial t} = -D \frac{\partial}{\partial z} \left\{ \frac{\partial n}{\partial z} + \frac{qN_0}{K_B T} \frac{\partial V}{\partial z} \right\} - kn \quad (\text{A3})$$

and

$$\frac{\partial^2 V}{\partial z^2} = -\frac{q}{\varepsilon} n, \quad (\text{A4})$$

that have to be solved with the boundary conditions

$$\frac{\partial n}{\partial z} + \frac{qN_0}{K_B T} \frac{\partial V}{\partial z} = 0 \quad (\text{A5})$$

for  $z = \pm d/2$ , related to the hypotheses of blocking electrodes, and  $V(\pm d/2, t) = \pm(V_0/2) \exp(i\omega t)$ , for the presence of the external power supply. Due to the linear character of the partial differential equations (A3) and (A4), the solutions we are looking for are of the type  $n(z, t) = \eta(z) \exp(i\omega t)$  and  $V(z, t) = \phi(z) \exp(i\omega t)$ , where for the symmetry of the problem under consideration,  $\eta(z) = -\eta(-z)$  and  $\phi(z) = -\phi(-z)$ . By substituting these expressions for  $n(z, t)$  and  $V(z, t)$  into Eqs. (A3) and (A4) and Eq. (A5) we get

$$\frac{i\omega + k}{D} \eta(z) = \eta''(z) + \frac{qN_0}{K_B T} \phi''(z), \quad (\text{A6})$$

and  $\phi''(z) = -(q/\varepsilon)\eta(z)$ , for the bulk equations, and

$$\eta'(z) + \frac{qN_0}{K_B T} \phi'(z) = 0, \quad (\text{A7})$$

and  $\phi(z) = \pm V_0/2$ , for the boundary conditions at  $z = \pm d/2$ . In Eqs. (A6) and (A7), the prime means derivative with respect to  $z$ . By substituting  $\phi''(z) = -(q/\varepsilon)\eta(z)$  into Eq. (A6), we get

$$\eta''(z) - \beta^2 \eta(z) = 0, \quad (\text{A8})$$

where

$$\beta = \frac{1}{\Lambda} \sqrt{1 + \kappa + i \frac{\omega}{\omega_D}}, \quad (\text{A9})$$

where  $\kappa = k/\omega_D$  is a dimensionless parameter related to the recombination phenomenon. Solution of Eq. (A8), with the symmetry  $\eta(z) = -\eta(-z)$  is  $\eta(z) = A \sinh(\beta z)$ , where  $A$  is an integration constant. By substituting  $\eta(z) = A \sinh(\beta z)$  into  $\phi''(z) = -(q/\varepsilon)\eta(z)$  and integrating we obtain

$$\phi(z) = -\frac{q}{\varepsilon \beta^2} A \sinh(\beta z) + Bz, \quad (\text{A10})$$

where  $B$  is another integration constant. The integration constants  $A$  and  $B$  are determined by the boundary conditions Eq. (A7) and  $\phi(\pm d/2) = \pm V_0/2$ . A simple calculation gives

$$A = -\frac{\varepsilon \beta^2}{q[\beta d(-1 + \beta^2 \Lambda^2) \cosh(\beta d/2) + 2 \sinh(\beta d/2)]} V_0,$$

$$B = \frac{\beta(-1 + \beta^2 \Lambda^2) \cosh(\beta d/2)}{\beta d(-1 + \beta^2 \Lambda^2) \cosh(\beta d/2) + 2 \sinh(\beta d/2)} V_0.$$

To evaluate the electric impedance of the cell, the calculation is now the usual one. The electric field in the cell is

given by  $E(z, t) = -\partial V/\partial z = -\phi(z)' \exp(i\omega t)$ , and the electric displacement by  $D(z, t) = \varepsilon E(z, t)$ . It follows that the electric current across the blocking electrode is  $I(t) = -SdD(d/2, t)/dt$ , where  $S$  is the surface area of the electrode. By taking into account Eq. (A10) a simple calculation gives

$$I(t) = -i\omega S \left( \frac{q}{\beta} A \cosh(\beta d/2) - \varepsilon B \right) \exp(i\omega t). \quad (\text{A11})$$

The impedance we are looking for, defined by  $Z = V_0 \exp(i\omega t)/I(t)$ , is found to be

$$Z = \frac{V_0}{-i\omega S[(q/\beta)A \cosh(\beta d/2) - \varepsilon B]}. \quad (\text{A12})$$

By substituting in Eq. (A12), the expressions for  $A$  and  $B$  reported above we get

$$Z = \frac{d\beta(-1 + \Lambda^2 \beta^2) + 2 \tanh(\beta d/2)}{i\varepsilon \Lambda^2 \omega \beta^3 S}, \quad (\text{A13})$$

that is the expression used for our numerical calculations.

## APPENDIX B: RENORMALIZED WAVE-VECTOR INVESTIGATION

Note that the presence of the G-R effect renormalizes the complex wave-vector  $\beta$ . It is possible to rewrite  $\beta$  as follows:

$$\beta = M[\cos(\psi/2) + i \sin(\psi/2)], \quad (\text{B1})$$

where

$$M(\omega) = \frac{1}{\Lambda} \{(1 + \kappa)^2 + (\omega/\omega_D)^2\}^{1/4} \quad (\text{B2})$$

and

$$\tan \psi(\omega) = \frac{\omega/\omega_D}{1 + \kappa}. \quad (\text{B3})$$

From Eq. (B2), we get that  $M$  is a monotonic increasing function of  $\omega$ , such that

$$\lim_{\omega \rightarrow 0} M = \frac{1}{\Lambda} \sqrt{1 + \kappa} \quad (\text{B4})$$

and for  $\omega \rightarrow \infty$ ,

$$\lim_{\omega \rightarrow \infty} M = \frac{1}{\Lambda} \sqrt{\frac{\omega}{\omega_D}}. \quad (\text{B5})$$

From Eq. (B3), it follows that  $\psi$  is monotonically increasing from 0 to  $\pi/2$ . The real part of  $\beta$ ,  $\beta_R$ , is such that  $\beta_R(0) = M(0)$ , whereas the imaginary part,  $\beta_I$ , is such that  $\beta_I(0) = 0$ . In the high frequency region,  $\omega \gg \omega_D$ ,

$$\lim_{\omega \rightarrow \infty} \beta_R = \lim_{\omega \rightarrow \infty} \beta_I = \frac{1}{\Lambda} \sqrt{\frac{\omega}{2\omega_D}}. \quad (\text{B6})$$

As it is evident from the discussion reported above, the presence of the L-source renormalizes  $\beta_0$  in  $\beta$ . In all the equations important for the analysis of the impedance of the cell, this means that the effect of the L-source is contained in the complex parameter defined by  $\beta = \alpha \beta_0$ , by means of which the standard formulas have to be rewritten. By taking into

account Eqs. (B1)–(B3) the real and imaginary parts of  $\alpha$  can be easily evaluated. In the limit of small  $\kappa$ , they are given by

$$\alpha_R = \text{Re}[\beta/\beta_0] = 1 + \frac{\kappa}{1 + (\omega/\omega_D)^2} + \mathcal{O}(\kappa^2), \quad (\text{B7})$$

$$\alpha_I = \text{Im}[\beta/\beta_0] = -\frac{\omega/\omega_D}{2[1 + (\omega/\omega_D)^2]} \kappa + \mathcal{O}(\kappa^3). \quad (\text{B8})$$

From Eq. (B7), it follows that  $\alpha_R(\omega)$  is a monotonic decreasing function, whereas from Eq. (B8) that  $\alpha_I(\omega)$  presents a minimum for  $\omega = \omega_D$ . For  $\omega = \omega_D$ , we get

$$\alpha_R(\omega_D) = 1 + \frac{\kappa}{2} \quad \text{and} \quad \alpha_I(\omega_D) = -\frac{\kappa}{4}. \quad (\text{B9})$$

<sup>1</sup>J. R. Macdonald, *Phys. Rev.* **92**, 4 (1953).

<sup>2</sup>E. M. Lifshitz and L. P. Pitaevskii, *Physical Kinetics*, Landau and Lifshitz Course of Theoretical Physics Vol. 10 (Butterworth–Heinemann, Oxford, 1997).

<sup>3</sup>J. R. Macdonald and D. R. Franceschetti, *J. Chem. Phys.* **68**, 1614 (1978).

<sup>4</sup>D. R. Franceschetti and J. R. Macdonald, *J. Appl. Phys.* **50**, 291 (1979).

<sup>5</sup>G. Derfel, E. Kaminski Lenzi, C. Refosco Yednak, and G. Barbero, *J. Chem. Phys.* **132**, 224901 (2010).

<sup>6</sup>G. Barbero and I. Lelidis, *J. Phys. Chem. B* **115**, 3496 (2011).

<sup>7</sup>J. Bisquert, *J. Phys. Chem. B* **106**, 325 (2002).

<sup>8</sup>F. Fabregat-Santiago, G. Garcia-Belmonte, J. Bisquert, A. Zaban, and P. Salvador, *J. Phys. Chem. B* **106**, 334 (2002).

<sup>9</sup>Q. Wang, J.-E. Moser, and M. J. Graetzel, *J. Phys. Chem. B* **109**, 14945 (2005).

<sup>10</sup>J. Villanueva-Cab, H. Wang, G. Oskam, and L. M. Peter, *Phys. Chem. Lett.* **1**, 748 (2010).

<sup>11</sup>K. Schwarzburg, R. Ernstorfer, S. Felber, and F. Willig, *Coord. Chem. Rev.* **248**, 1259 (2004).

<sup>12</sup>F. Fabregat-Santiago, J. Bisquert, E. Palomares, L. Otero, D. Kuang, S. M. Zakeeruddin, and M. Graetzel, *J. Phys. Chem. C* **111**, 6550 (2007).

<sup>13</sup>K. Ivan, N. Kischner, P. L. Simon, V. Jakab, Z. Noszticzius, J. H. Merkin, and S. K. Scott, *Phys. Chem. Chem. Phys.* **8**, 1339 (2002).

<sup>14</sup>G. Barbero and M. Scalerandi, *J. Chem. Phys.* **136**, 084705 (2012).

<sup>15</sup>G. Barbero and I. Lelidis, *Phys. Rev. E* **76**, 051501 (2007).

<sup>16</sup>G. Barbero, F. Batalioto, and A. M. Figueiredo Neto, *Appl. Phys. Lett.* **92**, 172908 (2008).

<sup>17</sup>G. Barbero and A. L. Alexe-Ionescu, *Liq. Cryst.* **32**, 943 (2005).

<sup>18</sup>G. Barbero, A. L. Alexe-Ionescu, and I. Lelidis, *J. Appl. Phys. Chem. B* **98**, 113703 (2005).

<sup>19</sup>P. W. Atkins, *Physical Chemistry*, 5th ed. (Oxford University Press, Oxford, 1994).

<sup>20</sup>J. R. Macdonald, *J. Phys.: Condens. Matter* **24**, 175004 (2012).